Enhanced cleaning of sink drains alters the bacterial community in plumbing components but not on countertop surfaces

Neil R. Gottel[1], Megan S. Hill[1], Shan Sun[2], Anthony A. Fodor[2], Bobby G. Warren[3,4], Deverick J. Anderson[3,4], Claudia K. Gunsch[1]

[1]Department of Civil and Environmental Engineering, Duke University, Durham, NC, USA;

[2]Department of Bioinformatics and Genomics, University of North Carolina at Charlotte, Charlotte, NC, USA

[3]Disinfection, Resistance, and Transmission Epidemiology (DiRTE) lab, Durham, NC, USA

[4]Duke Center for Antimicrobial Stewardship and Infection Prevention, Division of Infectious Diseases, Duke University Medical Center, Durham, NC, USA

Corresponding author: Claudia K. Gunsch, ckgunsch@duke.edu

Key words: sink microbiome, environmental reservoirs, healthcare-associated infections, bacterial colonization, hospital environment, pathogen transmission, antimicrobial resistance, longitudinal study, built environment

Abstract

Hospital sink drainage systems serve as reservoirs for healthcare-associated pathogens, yet the ecological mechanisms of effective antimicrobial control remain poorly understood. We conducted a 35-week longitudinal study comparing sink microbiomes in 30 hospital rooms treated with hydrogen peroxide-based, acid-mixture versus untreated controls. Using 16S rRNA sequencing of 1,957 samples from tail pieces, P-traps, and countertops, we characterized treatment effects on community structure and pathogen abundance. Treatment reduced genus richness by 50% in plumbing components but had no effect on the countertop. Critically, genera that contain ESKAPEE pathogens (*Klebsiella*, *Acinetobacter*, and *Enterobacter*) were significantly enriched in untreated sinks, while treated communities were dominated by soil- and water-associated bacteria, with *Bradyrhizobium* showing the strongest effect. Treatment created a "controlled instability" signature with reduced temporal autocorrelation and directional drift, disrupting biofilm succession without chaotic fluctuations. Treatment effects were detectable from week 1 and sustained throughout the study. Differential abundance analysis revealed 85% of treatment-enriched genera were environmental bacteria, indicating ecological replacement rather than sterilization. Our findings demonstrate that effective antimicrobial treatment establishes alternative community states that resist pathogen colonization while maintaining environmental responsiveness, challenging traditional sterilization-based approaches to healthcare environment management.

Importance

Hospital-acquired infections represent a major public health burden affecting millions annually. This study reveals that effective pathogen control operates through ecological replacement rather than sterilization. A hydrogen peroxide-based treatment established stable microbial communities dominated by environmental bacteria that consistently resist colonization by pathogen-containing groups, like *Klebsiella* and *Enterobacter*. Treatment effects were immediate and sustained over 35 weeks, indicating robust protection. Unlike traditional approaches that aim to eliminate all microbes, this ecological strategy maintains community responsiveness while preventing pathogen establishment. These findings demonstrate that carefully managed bacterial communities provide

sustainable pathogen control, offering a paradigm shift for healthcare environment management from broad suppression to targeted ecological intervention.

Introduction

Hospital-acquired infections (HAIs) pose a significant health risk, with 1 in 31 patients infected with an HAI daily, resulting in 72,000 deaths per year in the USA alone[1]. Many of these HAIs are caused by exposure to bacteria that are classified as ESKAPEE pathogens (*Enterococcus faecium*, *Staphylococcus aureus*, *Klebsiella pneumoniae*, *Acinetobacter baumannii*, *Pseudomonas aeruginosa*, *Enterobacter* spp., and *Escherichia coli*)[2]; a group that is characterized by their ability to form biofilms.[3] These biofilms increase bacterial survival, and they can serve as a reservoir for plasmids carrying antimicrobial resistance (AMR) genes[4], promoting AMR gene transfer[5]. Additionally, there is increased selection for biofilm-forming bacteria in more extreme environments, contributing to a greater diversity and prevalence of ESKAPEE-associated AMR genes in clinical settings when compared to their environmental counterparts[6,7]. This is of particular concern on surfaces that are difficult to access or clean with standard hospital sanitation methods, including plumbing components.

Hospital sinks are known hotspots for pathogen accumulation and dispersal in patient rooms[8,9], with studies showing that ICU rooms with sinks are associated with higher rates of HAIs compared to sink-free units[10]. The P-trap, in particular, functions as a primary pathogen reservoir. It retains standing water, providing a nutrient-rich, moist environment that supports biofilm establishment and microbial persistence[11,12]. Quantitative analyses have demonstrated that P-trap biofilms harbor significantly elevated concentrations of opportunistic pathogens, including *P. aeruginosa* and carbapenemase-producing Enterobacteriaceae, with bacterial densities exceeding 10^8 colony-forming units per surface area[12,13]. Further, P-trap biofilms exhibit active upward growth dynamics that enable pathogen translocation from the P-trap to more accessible drain components, such as the tail piece[11]. Although removal of sinks from patient rooms would likely reduce infection rates[10], this would require costly redesign and renovation of entire hospital units. Alternative methods might include heating the tail piece[14], using materials with antimicrobial properties (e.g., copper)[15], application of ozone[16], and the use of steam or boiling water[17].

However, these approaches can be costly or difficult to deploy at hospital-wide scales, necessitating tractable disinfection practices that target these locations.

New approaches use foaming agents combined with disinfectants, such as hydrogen peroxide and peroxyacetic acid, to prolong contact time with the treated surface. This has been shown to effectively reduce colonization by gram-negative bacteria[18], opportunistic premise plumbing pathogens (OPPPs)[19], and epidemiologically important pathogens (EIPs)[20]. Here, we applied an antimicrobial foaming agent to hospital sinks in patient rooms at Duke University Hospital within a newly renovated intermediate care unit (IMCU); a unit that houses patients that require a care-level between general patient care and the ICU. Prior to cleaner application and sample collection, plumbing components were installed and rooms had not yet been occupied by patients. For half of the sinks, a foaming hydrogen peroxide/peracetic acid solution was applied to the sink tail piece three times per week (Monday, Wednesday, Friday), and samples were collected one day per week (Tuesday) from three locations, including the tail piece, P-trap, and countertop. We then sequenced the full-length 16S rRNA gene to assess differences in bacterial community dynamics at different temporal and spatial scales. Additionally, we examined how observed changes in community structure influenced the relative abundance of bacteria of concern and identified taxa that are negatively correlated with ESKAPEE bacteria to determine potential targets for bioremediation efforts to reduce exposure and infection risk.

Methods

Study Design

The study was conducted in a newly renovated IMCU at Duke University Hospital; a 1048-bed tertiary care hospital located in Durham, North Carolina, USA, as previously described[20]. Sink-associated samples were collected from the P-trap, tail piece, and countertop of 30 sinks over a 35-week period, starting in July of 2024. Samples were collected once per week (Tuesday), and collection began one week prior to patient occupation. Of the 30 rooms, half were randomly selected to receive an enhanced cleaning intervention three times a week (Monday, Wednesday, Friday). The enhanced cleaning product, Virasept (Ecolab, # 6002314), is a peroxide-based, acid-mixture liquid with three key active ingredients: hydrogen peroxide (3.13%), peroxyacetic acid (0.05%), and octanoic acid (0.099%). Virasept is sold as a liquid product, but when pumped

through an applicator, forms a foam that remains within the tail piece for at least 5 minutes. Throughout the study duration, all rooms were cleaned per the standard hospital cleaning procedure, which includes daily surface disinfection with non-bleach solutions.

Sample collection and processing

Tail piece samples were collected using a Copen ESwab (BD, # 220245) that was inserted through the sink drain and rubbed against the internal surface of the tail piece, while applying pressure and rotating. The swab was transferred into the storage medium to elute the sample and was centrifuged at 10,000 x g for 1 minute to pellet the cells. The resulting cell pellet was transferred to a lysis tube. P-trap samples were collected using a syringe and tubing. The syringe was pumped several times to resuspend settled particles and 15 mL of liquid was retained. This liquid was vacuum filtered through a 0.22-micron filter (Omicron Scientific, # 170047) on a fritted glass support base. The filter was shredded with flame sterilized scissors and tweezers, then inserted into a PowerSoil Pro (Qiagen, # 47126) lysis tube. Lastly, countertop samples were collected using a cellulose sponge pre-moistened in phosphate buffered saline with 1% Tween 20. Following collection, the sponge was processed using the stomacher technique in accordance with the Centers for Disease Control and Prevention protocol[21]. After collection, sponges were placed in stomacher bags with 45 mL of phosphate-buffered saline with 1% Tween 20 and then homogenized for 60 seconds at 260 rpm. Homogenates were then centrifuged at 10,000 x g for 10 minutes. The supernatant was removed, and the pellet was collected with a sterile cotton swab (Puritan, # 806-WC). The tip of the cotton swab was then cut off into a PowerSoil Pro lysis tube. All samples were stored at -20°C until DNA extraction.

DNA extraction and sequencing

DNA was extracted following the manufacturer's instructions with the DNeasy PowerSoil Pro kit (QIAGEN) and quantified using a Qubit dsDNA BR Assay Kit (Thermo Fisher, # Q32853). Samples with DNA concentrations > 1 ng/µl were normalized to 1 ng/µl; samples below this threshold were not normalized. A 2 µl aliquot of each sample was then subjected to PCR amplification of the full-length 16S rRNA gene following the PacBio Kinnex 16S kit protocol

(PacBio), using Phusion Plus PCR Master Mix (Thermo Fisher Scientific, # F631L) and 27F - 1492R universal primer pair (5'-AGRGTTYGATYMTGGCTCAG-3' and 5'-RGYTACCTTGTTACGACTT-3', respectively). Primers with unique barcodes and Kinnex adaptor sequences were used at a final concentration of 0.3 µM. Reaction mixes were denatured for 30 seconds at 98°C prior to 30 cycles of denaturation at 98°C for 10 seconds, annealing at 57°C for 20 seconds, and extension at 72°C for 75 seconds. After the last cycle, a final extension at 72°C for 5 minutes was performed. Completed PCR reactions were visualized on an E-Gel (Invitrogen) to ensure that amplicon size was correct (~1500bp), and that each sample amplified appropriately. Amplicon libraries were subsequently pooled at different volumes, based on gel band intensity (1, 2.5, 5, 10, or 20 µl per reaction). The pooled libraries were cleaned and concentrated using 1.1X volume of SMRTbell® cleanup beads (PacBio) and eluted in 50 µl of low TE elution buffer (PacBio). Cleaned libraries were stored at -20°C prior to Kinnex PCR for concatenation and circularization. Kinnex PCR was performed as outlined in the PacBio Kinnex 16S kit's published protocol with no modifications (PacBio). Size selected and cleaned libraries were loaded onto a PacBio SMRT® Cell and sequenced on the Revio system (PacBio) at the Duke Sequencing and Genomic Technologies (SGT) Shared Resource facility.

Data analysis

Circular consensus sequencing (CCS) data were quality filtered (Q20), de-concatenated, demultiplexed, and converted from .bam to .fastq format in the SMRT Link software system (PacBio). Barcode and adapter sequences were removed using the q2-demux plugin[22]. Demultiplexed full-length 16S rRNA amplicon sequences were analyzed with DADA2[22] and QIIME2[23] following the developers' instructions. Denoising, dereplication, ASV inference, and chimera removal were performed with the DADA2 long-read pipeline. Taxonomy was assigned with QIIME2 feature classifier using the GTDB database (release 220)[24]. Abundance values were normalized by multiplying the relative abundance by the average sequencing depth, as previously described[25]. Statistical analyses were performed in R (v. 4.3.1)[26].

Community turnover was quantified as the week-to-week Bray-Curtis dissimilarity between consecutive sampling timepoints within each room and sampling location. For each room, all adjacent timepoint pairs were identified by sorting samples by week, and the mean pairwise

dissimilarity was calculated as a per-room turnover score. Differences in turnover between treated and untreated sinks were tested by Wilcoxon rank-sum test within each sampling location. To assess when treatment effects emerged over the study period, a per-week PERMANOVA was performed for each week that had sufficient paired samples, using treatment as the predictor variable within each sampling location.

Community instability was characterized using three complementary approaches, all based on Aitchison distance. First, per-room volatility was quantified as the mean step distance between consecutive weekly samples. Second, temporal autocorrelation was assessed by computing the lag-1 Pearson autocorrelation of each room's distance-from-centroid time series, where the centroid was defined as the mean CLR vector across all timepoints for that room; rooms with fewer than four timepoints were excluded. A positive lag-1 autocorrelation (ACF) indicates that the community exhibits temporal dependence over time, while a value near zero indicates unpredictable week-to-week dynamics. Third, per-room PERMANOVA R^2 was calculated by fitting week as the sole predictor of Aitchison distances within each room, where high R^2 indicates directional community drift over time and low R^2 indicates a stable or randomly fluctuating community. Differences in volatility, ACF, and PERMANOVA R^2 between treatment groups were tested by Wilcoxon rank-sum tests for each sampling location.

Alpha diversity was assessed using the Chao1 richness estimator and Shannon diversity index. Differences in alpha diversity between treated and untreated sinks were tested separately for each sampling location (tail piece, P-trap, countertop) using Wilcoxon rank-sum tests with Benjamini-Hochberg correction for multiple comparisons. Beta-diversity was calculated using Aitchison distance, calculated using a centered log-ratio (CLR) transformation with a half-minimum pseudocount and Euclidean distance[27]. Differences in bacterial community profiles between treatment groups were tested using PERMANOVA with the 'adonis2' function with 999 permutations and strata set to room to account for the paired room-level treatment design[28]. Beta-dispersion (homogeneity of within-group variance) was assessed using the 'betadisper' function in vegan[28], and variance partitioning was performed using the 'varpart' function on Hellinger-transformed community matrices, to quantify the independent contributions of treatment, sample type, week, and room to community composition[29].

Differential abundance of individual taxa between treated and untreated sinks was assessed using ALDEx2[30] with Welch's t-test and Wilcoxon rank-sum test, using 128 Monte Carlo Dirichlet instances to propagate compositional uncertainty. Taxa present in fewer than 5% of samples within an individual sampling location were excluded. Effect sizes are reported as the difference between the group median log-ratio abundances, and significance was assessed using Benjamini-Hochberg-corrected p-values from both the parametric and non-parametric tests. A negative effect size is enrichment in the treated samples, whereas a positive effect is enrichment in the control samples.

To characterize the ecological niches frequently occupied by the differentially abundant taxa, genera identified to be significant were classified into functional groups: oligotrophic environmental bacteria (soil rhizobia and alphaproteobacterial water-associated taxa), disinfectant-tolerant bacteria, transient human commensals (skin- and oral-associated taxa), mature biofilm specialists (*Sphingomonadales* and co-occurring pipe biofilm community members), and clinically relevant groups (ESKAPEE pathogens). Indicator species analysis was performed using the 'multipatt' function in the indicspecies package[31] with 999 permutations to identify genera significantly associated with treated or untreated sinks within each sampling location. Co-occurrence networks were constructed for P-trap samples using Spearman correlations between genera recovered from at least 20% of samples, retaining edges with $|r| > 0.3$ and Benjamini-Hochberg-corrected $p < 0.05$, and network properties were compared, to assess whether treatment disrupts co-occurrence structure.

Results

Community Volatility and Instability Analysis

Overall, bacterial community volatility did not differ significantly between the treated and untreated sinks for all three locations (Fig. 1A, Aitchison distance: tail piece $P = 0.362$, P-trap $P = 0.709$, countertop $P = 0.340$). However, week-to-week compositional change revealed complex temporal dynamics (Fig. 1B). There were statistically significant differences between treatment groups, with 19 of 34 weeks in tail piece samples, 14 of 34 weeks showing variation in P-trap samples, and only 1 of 34 weeks in countertop samples (Table S1; Wilcoxon rank-sum tests, $P < 0.05$). The weeks that exhibited community volatility occurred sporadically throughout the study period with no consistent patterns or directionality. Temporal clustering of significant weeks (e.g.,

weeks 21-26) could suggest small, but consistent, treatment-specific responses to facility-wide environmental conditions, evidenced by overlapping confidence intervals that nonetheless yielded statistically significant differences due to consistent separation of underlying room-level distributions (Fig. 1A, Table S1).

Complementary analysis of temporal stability patterns revealed that treated bacterial communities had altered ecological dynamics compared to untreated communities. Lag-1 temporal autocorrelation analysis showed that tail piece communities displayed significantly lower week-to-week predictability than those from untreated samples ($W = 62$, $P = 0.038$), with treated communities exhibiting near-zero autocorrelation (-0.06) compared to positive autocorrelation in untreated communities (0.16) (Fig. 2A). No significant differences were found in the P-traps ($P = 0.590$) or on countertops ($P = 0.967$), with the countertops having a high ACF in both groups (~0.35). Additionally, per-room PERMANOVA analysis showed that temporal drift patterns differed between treatments, with the week of study explaining significantly less compositional variance in treated communities (tail piece: 6-8% variance, significant in 7-20% of rooms) compared to untreated sinks (11% variance, significant in 80-87% of rooms) (Fig. 2B, $P < 0.0001$). Similarly, in P-traps, treatment explained 5-7% variance based on week of sample collection (significant in 15-25% of rooms), compared to 10-12% variance in untreated sinks (significant in 75-85% of rooms) ($P = 0.011$). There was no reduction in temporal drift among treated communities for countertop samples (Fig. 2B, $P = 0.481$).

Joint analysis of autocorrelation and directional drift patterns showed distinct temporal stability dynamics. Treated communities, which clustered predominantly in the lower-left quadrant of the ACF vs R^2 space (Fig. 2C), were characterized by low temporal predictability and minimal directional drift. This controlled instability signature was most pronounced in plumbing components, with minimal overlap of untreated communities in tail piece and P-trap samples, but not among countertops. Group centroids (diamond markers) confirmed that treated plumbing communities have a distinct signature that is characterized by disrupted week-to-week predictability (low ACF) combined with reduced long-term directional change (low R^2). These results were reflected in species diversity and taxonomic compositional assessments.

Community Richness and Diversity

Treated tail pieces and P-traps had significantly less richness (Chao1: $P < 0.001$), with nearly half the average number of predicted genera (Fig. 3A, treated: tail piece = 13.5, P-trap = 25.1; untreated: tail piece = 25.4, P-trap = 41.3). Consistent with our other findings, there was no observable effect on richness among countertop samples ($P = 0.211$). When evenness was considered, treated P-traps had significantly lower diversity (Shannon: $P = 0.0026$), but there were no differences in tail pieces or on countertops (Fig. 3A, Shannon: $P = 0.573$ and $P = 0.330$, respectively).

Additionally, there were differences in the overall community structure between treated and untreated samples from tail pieces and P-traps ($P = 0.001$ for both), with no observable differences at the countertop locations ($P = 0.180$) (Fig. 3B), despite frequent identification of the most abundant taxa across all three surfaces. These included common sink-associated bacteria (e.g., *Pseudomonas*, *Spingomonas*, *Cupriavidus*), body associates (e.g., *Staphylococcus*, *Veillonella*), and environmentally-sourced groups (e.g., *Bradyrhizobium*, *Methylobacterium, Novosphingobium*) (Fig. 4). Therefore, to further assess which taxa were driving the observed differences in community membership, a differential abundance analysis was performed.

Differentially Abundant Taxa

Based on treatment, there were 22 significant genera in tail pieces and 41 significant genera in P-traps, while no genera were significantly differentially abundant among countertops (Fig. 5, Table 1). Additionally, there was a strong positive correlation between tail piece and P-trap responses ($r = 0.611$, $P < 0.001$) that demonstrated consistent, rather than stochastic, changes in the community-level response.

Treated-enriched genera were predominantly soil- and water-associated bacteria (~85%), including nitrogen-fixing rhizosphere bacteria (*Bradyrhizobium*, *Mesorhizobium*), spore-forming soil bacteria (*Bacillus*, *Sporosarcina*, *Paenibacillus*), environmental actinobacteria (*Rhodococcus*), and freshwater-associated taxa (*Pelomonas*). *Bradyrhizobium* had the strongest enrichment in treated samples across both locations (tail piece: effect = -0.801, $P < 0.0001$; P-trap: effect = -0.625, $P < 0.0001$), along with other environmental taxa, such as *Afipia* (a plant-associated Alphaproteobacteria, effect = -0.459 to -0.151) and *Mycobacterium* (Table 1).

Conversely, untreated samples were significantly enriched for genera that contain opportunistic and pathogenic taxa, particularly members of the ESKAPEE group. Although species-level identification was not possible within the scope of this study, *Klebsiella*, *Enterobacter*, and *Acinetobacter* showed consistent enrichment in untreated communities across both plumbing locations (all $P < 0.01$), with effect sizes ranging from 0.130 to 0.366 (Fig. 5, Table 1). *Sphingomonas*, *Comamonas*, *Agrobacterium*, and *Chryseobacterium* were also enriched, which represent bacteria adapted to nutrient-rich environments typical of biofilms that are formed in untreated plumbing systems.

Discussion

Our characterization of temporal dynamics, community structure, and taxonomic composition in hospital sinks suggests that enhanced cleaning using hydrogen peroxide, peracetic acid, treatment increases infection control through community-level disturbance and ecological replacement, rather than broad bacterial suppression. Observable effects were restricted to plumbing components (tail pieces and P-traps), demonstrating that Virasept imposes localized selection pressures that restructure bacterial communities at the site of application and immediate adjacent locations. This could be due to a limited contribution of bacteria from sinks to countertops relative to inputs from air and room occupants[32,33]. Cleaner application results in reduced temporal predictability and directional drift that disrupts normal biofilm successional patterns, while maintaining consistent compositional responses to environmental perturbations. Most significantly, the treatment consistently favors soil- and water-associated bacteria (~85% of enriched taxa) over healthcare-associated pathogens, creating stable alternative community states dominated by nitrogen-fixing rhizosphere bacteria, spore-forming environmental taxa, and stress-tolerant Actinobacteria. The strong correlation between tail piece and P-trap responses ($r = 0.611$, $P < 0.001$), coupled with the suppression of ESKAPEE pathogens across both locations, indicates that enhanced cleaning alters community dynamics potentially allowing for competitive exclusion rather than stochastic antimicrobial effects. These findings challenge conventional approaches to environmental disinfection by demonstrating that targeted environmental manipulation can alter ecological dynamics in ways that provide pathogen control through the establishment of environmentally beneficial bacteria.

Although overall community volatility was similar between treatments, temporal dynamics diverged in ways that reveal a more nuanced treatment effect (Fig. 1). Treated tail piece communities showed reduced week-to-week predictability (lag-1 ACF = −0.06 vs. 0.16 in untreated samples), indicating that treatment suppresses biofilm-forming taxa in favor of more transient species. Treated communities consistently clustered in a low-autocorrelation, low-drift quadrant, reflecting what we term controlled instability — treatment prevents normal biofilm successional patterns without generating stochastic fluctuations (Fig. 2). This distinguishes the treatment effect from simple destabilization and instead suggests an alternative resilience dynamic in which communities remain responsive to environmental perturbations but cannot establish the predictable successional trajectories characteristic of untreated sinks. In P-traps, the response was less strong. Treatment significantly reduced R^2 but did not alter the ACF, suggesting that there was only partial community disruption (Fig. 2). This likely reflects physical and ecological features of P-traps, which continually retain liquid and might receive elevated nutrient inputs depending on sink use, supporting greater biofilm development. Dilution of the cleaner in the P-trap liquid could be an additional factor, reducing its efficacy relative to the tail piece location. This has implications for pathogen control and disease prevention within the hospital, since the tail piece can be rapidly colonized by bacteria in the P-trap if enhanced cleaning is applied infrequently, or if regular use is halted. Integration of volatility and stability analyses demonstrated that treatment effects operate through controlled ecological disruption rather than community destabilization. The combination of consistent weekly volatility responses (small effect sizes with statistical significance due to tight distributions) and altered temporal stability patterns (disrupted autocorrelation and drift) indicate that Virasept treatment maintains dynamic community responsiveness while preventing the establishment of predictable biofilm successional patterns that are typical of untreated sinks.

These differences were further reflected in the bacterial community diversity and composition. There were significant decreases in predicted richness within treated tail pieces and P-traps, with no differences among countertops (Fig. 3A). This may be due to the removal of rare species or selection for stress-tolerant taxa that are able to survive enhanced cleaning regimes. There was also a divergence in community membership for both plumbing sites (Fig. 3B). Although many of the highly abundant taxa were shared between all locations (Fig. 4), there was a consistent decrease in clinically relevant taxa and targeted ecological filtering.

Differential abundance analysis identified twice the number of differentially abundant genera in the P-traps (n=41) versus the tail pieces (n=22) (Table 1). This is counterintuitive given that the foaming agent targets the tail piece directly, but likely reflects the persistence of active disinfectant compounds in the P-trap after the foam dissipates and drips down — even in diluted form, prolonged contact time may amplify cumulative effects on P-trap communities, potentially damaging biofilms and planktonic cells. Across both sites, treatment consistently suppressed clinically relevant taxa, including multiple genera with ESKAPEE pathogens exhibiting effect sizes > 0.2, indicating substantial suppression in treated environments (*Enterobacter*, *Klebsiella*, and *Acinetobacter*) (Fig. 5). With this decrease, there was a corresponding increase in environmental bacteria. *Bradyrhizobium* showed the largest treatment effect (|effect| > 0.6), representing an approximate 4-7 $\log_2$ fold difference in abundance between treatments (Fig. 5). Generally, enriched genera were broadly characteristic of soil and water environments, including nitrogen-fixing (*Mesorhizobium*), biodegradation-associated (*Rhodococcus*), spore-forming (*Bacillus*, *Paenibacillus*), and freshwater (*Pelomonas*) taxa (Table 1). These organisms are slow growing, stress tolerant, and are adapted to oligotrophic conditions, suggesting that Virasept treatment creates selective pressures that favor environmental bacteria over hospital-adapted pathogens through oxidative stress and nutrient limitation. Whether this constitutes true competitive exclusion or simply improved detection of previously masked taxa due to reduced background community abundance remains unknown.

A parallel culture-based analysis of the same samples observed a significantly higher number of EIPs in samples from the untreated sinks[20], including *Acinetobacter*, *Enterobacter*, and *Klebsiella* species, with *P. aeruginosa* as the only isolate identified to the species level. Few EIPs were detected in countertop samples, resulting in mostly non-significant differences in detection between the control and treatment groups. This result mirrors the non-significant differences in the countertop bacterial community that we observed in the sequencing results. Importantly, *P. aeruginosa* and *Stenotrophomonas spp.* were significantly reduced, an outcome our sequencing-based approach was unable to detect. Future work would benefit from absolute quantification via spike-in extraction controls, and from higher-resolution tools such as metagenomics or digital PCR to identify clinically relevant genomic features and pathogenic strains.

The taxonomic composition of differentially abundant genera supports the hypothesis that effective environmental disinfection should aim for ecological replacement rather than sterile

elimination. The predominance of soil- and water-associated bacteria (~85% of treated-enriched taxa) demonstrates that Virasept treatment creates environmental conditions that consistently favor outdoor bacteria over hospital-adapted pathogens. The enrichment of functionally diverse environmental taxa indicates successful establishment of a stable, pathogen-resistant bacterial community with maintained ecosystem functioning. This ecological approach to infection control leverages competitive displacement, whereby environmentally adapted bacteria outcompete hospital-associated pathogens through adaptation to oxidative stress and nutrient limitation imposed by treatment regimens.

Acknowledgments

This work was supported primarily by the Engineering Research Centers Program of the National Science Foundation under NSF Cooperative Agreement No. EEC-2133504. We thank the Duke University School of Medicine for the use of the Microbiome Core Facility, which provided library preparation services, and for the use of the Sequencing and Genomics Core Facility which provided PacBio full-length 16S sequencing services. Purchase of the PacBio Revio was funded by the NIH (1S10OD034222-01). We thank Duke Hospital for their coordination and support of this project, and the members of the Duke Center for Antimicrobial Stewardship and Infection Prevention who helped collect samples and administer enhanced cleaning: Amanda M. Graves, Guerbine Fils-Aime, Aaron Barrett, Isadora Mamikunian, and Becky A. Smith.

Conflict of Interest

The authors have no conflicts of interest to declare.

Data Availability

Raw sequence files and metadata are publicly available in the National Center for Biotechnology Information (NCBI) Sequence Read Archive (SRA), under BioProject ID: PRJNA1433472. Additionally, preprocessing and analysis scripts are available on GitHub at https://github.com/hillms/hospital_sink_disinfection

References

1. CDC. HAIs: Reports and Data. *Healthcare-Associated Infections (HAIs)* https://www.cdc.gov/healthcare-associated-infections/php/data/index.html (2024).
2. Woh, P. Y. & Zhang, X. The burden of ESKAPE pathogen-related hospital-acquired infections: clinical and financial perspective from a systematic review. *J. Hosp. Infect.* **162**, 377–385 (2025).
3. Chong, C. S. C., Lau, Y. Y., Michels, P. A. M. & Lim, C. S. Y. Insights into biofilm-mediated mechanisms driving last-resort antibiotic resistance in clinical ESKAPE pathogens. *Crit. Rev. Microbiol.* **51**, 1081–1106 (2025).
4. Røder, H. L. *et al.* Biofilms can act as plasmid reserves in the absence of plasmid specific selection. *NPJ Biofilms Microbiomes* **7**, 78 (2021).
5. Djermoun, S. *et al.* Biofilm architecture determines the dissemination of conjugative plasmids. *Proc. Natl. Acad. Sci. U. S. A.* **122**, e2417452122 (2025).
6. Santajit, S. & Indrawattana, N. Mechanisms of antimicrobial resistance in ESKAPE pathogens. *Biomed Res. Int.* **2016**, 2475067 (2016).
7. Domingues, C. P. F., Rebelo, J. S., Dionisio, F. & Nogueira, T. Clinical and environmental plasmids: Antibiotic resistance, virulence, mobility, and ESKAPEE pathogens. *Antibiotics (Basel)* **15**, 29 (2025).
8. Gestrich, S. A. *et al.* A multicenter investigation to characterize the risk for pathogen transmission from healthcare facility sinks. *Infect. Control Hosp. Epidemiol.* **39**, 1467–1469 (2018).
9. Volling, C. *et al.* Are sink drainage systems a reservoir for hospital-acquired Gammaproteobacteria colonization and infection? A systematic review. *Open Forum Infect. Dis.* **8**, ofaa590 (2021).
10. Fucini, G.-B. *et al.* Sinks in patient rooms in ICUs are associated with higher rates of hospital-acquired infection: a retrospective analysis of 552 ICUs. *J. Hosp. Infect.* **139**, 99–105 (2023).
11. Kotay, S., Chai, W., Guilford, W., Barry, K. & Mathers, A. J. Spread from the sink to the patient: In situ study using green fluorescent protein (GFP)-expressing Escherichia coli

to model bacterial dispersion from hand-washing sink-trap reservoirs. *Appl. Environ. Microbiol.* **83**, (2017).

12. Healy, H. G. *et al.* Bacterial recolonization of hospital sink biofilms. *J. Hosp. Infect.* **162**, 95–105 (2025).

13. Franco, L. C. *et al.* A microbiological survey of handwashing sinks in the hospital built environment reveals differences in patient room and healthcare personnel sinks. *Sci. Rep.* **10**, 8234 (2020).

14. Park, S. *et al.* Some like it hot: Variable impact of a tailpiece heating device on different gram-negative bacteria. *Antimicrob. Steward. Healthc. Epidemiol.* **3**, s70–s70 (2023).

15. Gomes, I. B., Simões, M. & Simões, L. C. Copper surfaces in biofilm control. *Nanomaterials (Basel)* **10**, 2491 (2020).

16. Pajak-Zajac, M. Z., Dowdell, A., Potts, H. E., Smith, A. & Diver, D. A. Drain decontamination using in-situ-generated ozone. *J. Hosp. Infect.* **159**, 100–105 (2025).

17. Bourdin, T. *et al.* Disinfection of sink drains to reduce a source of three opportunistic pathogens, during Serratia marcescens clusters in a neonatal intensive care unit. *PLoS One* **19**, e0304378 (2024).

18. Jones, L. D. *et al.* Effectiveness of foam disinfectants in reducing sink-drain gram-negative bacterial colonization. *Infect. Control Hosp. Epidemiol.* **41**, 280–285 (2020).

19. Newcomer, E. P. *et al.* The effects of a prospective sink environmental hygiene intervention on Pseudomonas aeruginosa and Stenotrophomonas maltophilia burden in hospital sinks. *EBioMedicine* **116**, 105772 (2025).

20. Warren, B. G. *et al.* Efficacy of a foamed disinfectant in reducing pathogen contamination in renovated inpatient in-room sinks: a randomized controlled trial. *Infect. Control Hosp. Epidemiol.* 1–7 (2025).

21. ISO 11737-1:2018. *ISO* https://www.iso.org/standard/66451.html (2024).

22. Callahan, B. J. *et al.* DADA2: High-resolution sample inference from Illumina amplicon data. *Nat. Methods* **13**, 581–583 (2016).

23. Bolyen, E. *et al.* Reproducible, interactive, scalable and extensible microbiome data science using QIIME 2. *Nat. Biotechnol.* **37**, 852–857 (2019).

24. Parks, D. H. *et al.* GTDB release 10: a complete and systematic taxonomy for 715 230 bacterial and 17 245 archaeal genomes. *Nucleic Acids Res.* **54**, D743–D754 (2026).
25. Jones, R. B. *et al.* Inter-niche and inter-individual variation in gut microbial community assessment using stool, rectal swab, and mucosal samples. *Sci. Rep.* **8**, 4139 (2018).
26. R Core Team. *R: A Language and Environment for Statistical Computing*. (R Foundation for Statistical Computing, Vienna, Austria, 2024).
27. Martino, C. *et al.* A novel sparse compositional technique reveals microbial perturbations. *mSystems* **4**, (2019).
28. Community Ecology Package [R package vegan version 2.7-2]. *Comprehensive R Archive Network (CRAN)* https://CRAN.R-project.org/package=vegan (2025).
29. Legendre, P. & Gallagher, E. D. Ecologically meaningful transformations for ordination of species data. *Oecologia* **129**, 271–280 (2001).
30. Fernandes, A. D., Macklaim, J. M., Linn, T. G., Reid, G. & Gloor, G. B. ANOVA-like differential expression (ALDEx) analysis for mixed population RNA-Seq. *PLoS One* **8**, e67019 (2013).
31. De Cáceres, M. & Legendre, P. Associations between species and groups of sites: indices and statistical inference. *Ecology* **90**, 3566–3574 (2009).
32. Qian, J., Hospodsky, D., Yamamoto, N., Nazaroff, W. W. & Peccia, J. Size-resolved emission rates of airborne bacteria and fungi in an occupied classroom. *Indoor Air* **22**, 339–351 (2012).
33. Hospodsky, D. *et al.* Characterizing airborne fungal and bacterial concentrations and emission rates in six occupied children's classrooms. *Indoor air* **25**, (2015).

Figures

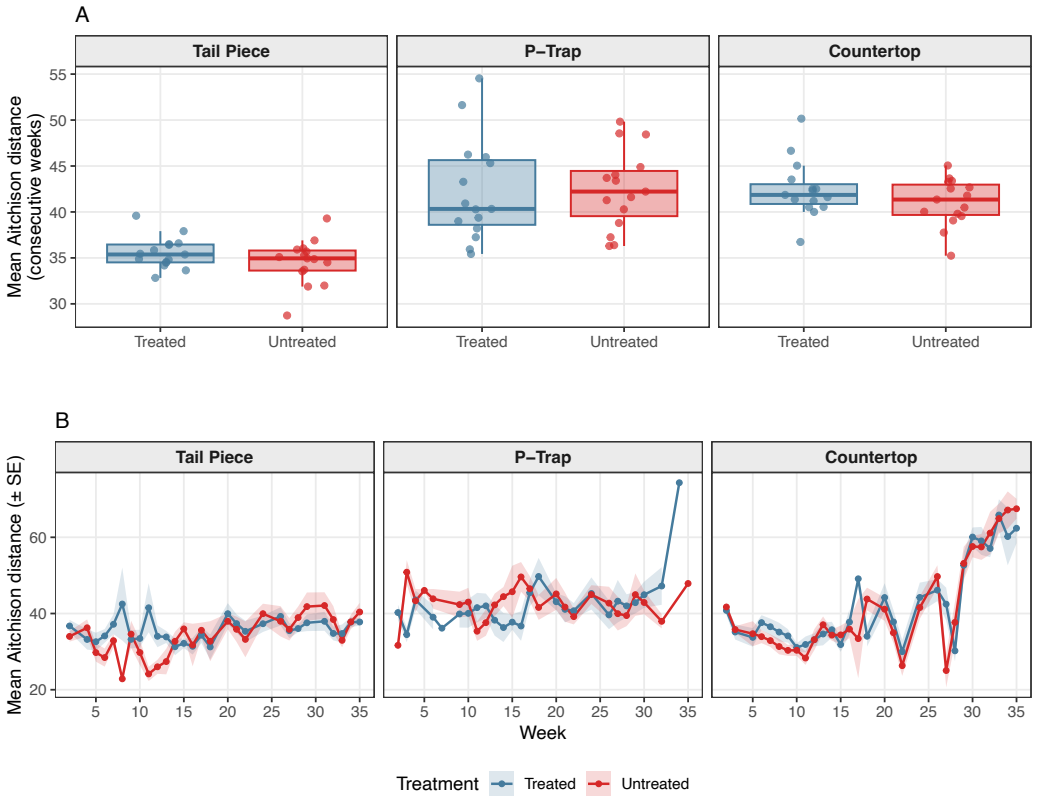

Figure 1. Bacterial community volatility by treatment and location in hospital sinks. Week-to-week compositional change using Aitchison distances on genus-level relative abundances comparing treated (blue) and untreated (red) samples across three locations. (A) Overall community volatility, in which each point represents the mean Aitchison distance between consecutive weeks for a single room. Higher values indicate greater compositional turnover between consecutive sampling timepoints. (B) Weekly volatility trajectories showing temporal patterns of community change over the 35-week study period. Points represent mean Aitchison distances between consecutive weeks across all rooms within each treatment-location combination. Shaded regions indicate standard error.

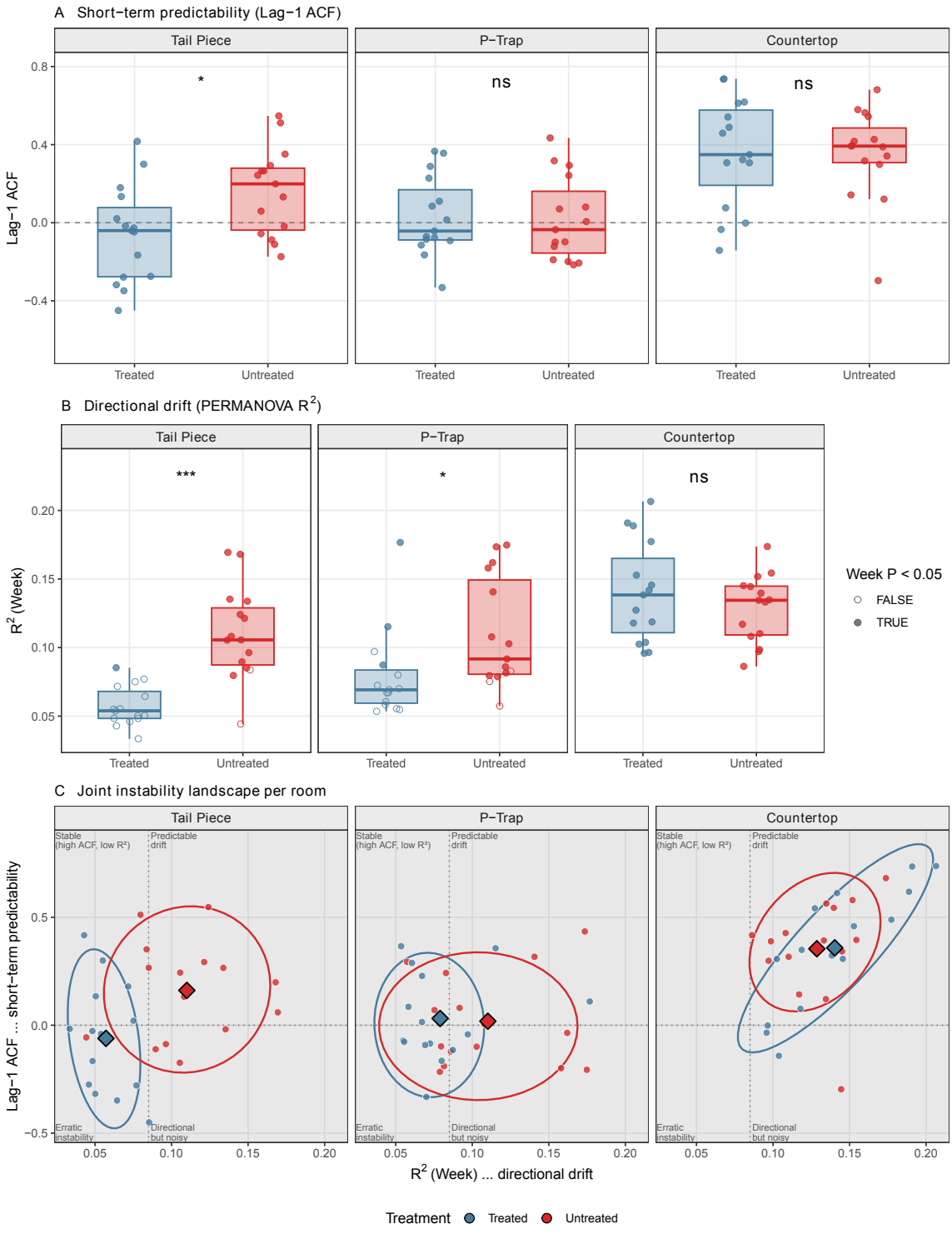

Figure 2. Bacterial community instability and temporal dynamics by treatment and location in hospital sinks. Analysis based on centered log-ratio (CLR) transformed genus-level relative abundances for treated (blue) and untreated (red) samples, with points representing individual rooms. Temporal autocorrelation computed from Euclidean distances

between each timepoint and the room-specific centroid. PERMANOVA performed on Aitchison distances. Rooms with ≥ 4 timepoints for ACF analysis and ≥ 5 timepoints for PERMANOVA were included. (A) Short-term predictability measured by lag-1 temporal autocorrelation (ACF) of distance-from-centroid time series. Values near 1 indicate highly predictable week-to-week patterns; values near 0 indicate erratic temporal fluctuations. Dashed horizontal line indicates ACF = 0. Statistical significance tested with Wilcoxon rank-sum tests. (B) Directional drift quantified by PERMANOVA R^2 values measuring the proportion of community variance explained by sampling week within each room. Higher R^2 indicates stronger temporal drift patterns; lower R^2 indicates stable or randomly fluctuating communities. Filled circles indicate significant week effects ($P < 0.05$) and open circles indicate non-significant effects. Statistical significance tested with Wilcoxon rank-sum tests. (C) Joint instability landscape plotting autocorrelation against directional drift for each room. Background quadrants provide ecological interpretation: upper-left = stable communities; upper-right = predictable directional drift; lower-left = erratic instability; lower-right = directional but unpredictable change. Dotted reference lines indicate median values across the dataset. 80% confidence ellipses indicate group clustering patterns; diamond markers indicate group centroids.

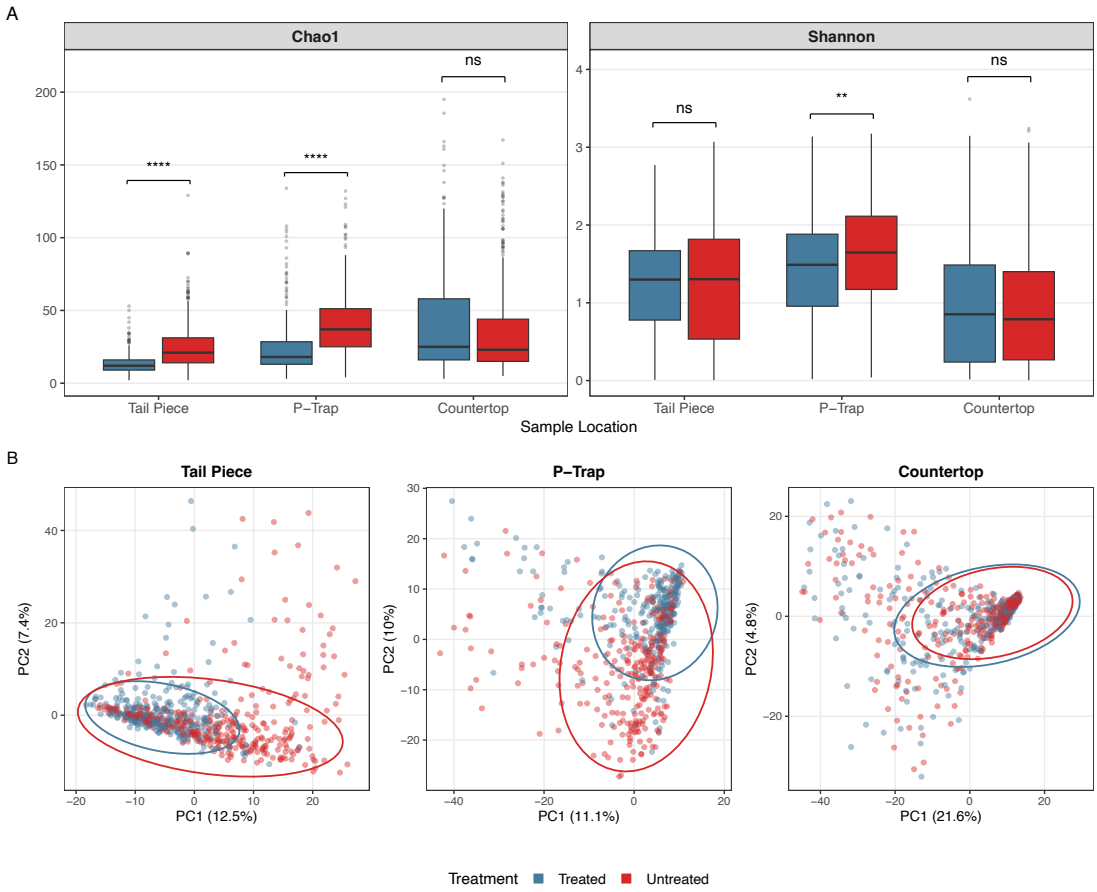

Figure 3. Alpha and beta diversity analysis of bacterial communities in hospital sink samples. (A) Alpha diversity metrics comparing treated (blue) and untreated (red) samples across three locations. (B) Principal coordinate analysis (PCoA) of Aitchison distances between bacterial communities. Ellipses represent 95% confidence intervals around group centroids.

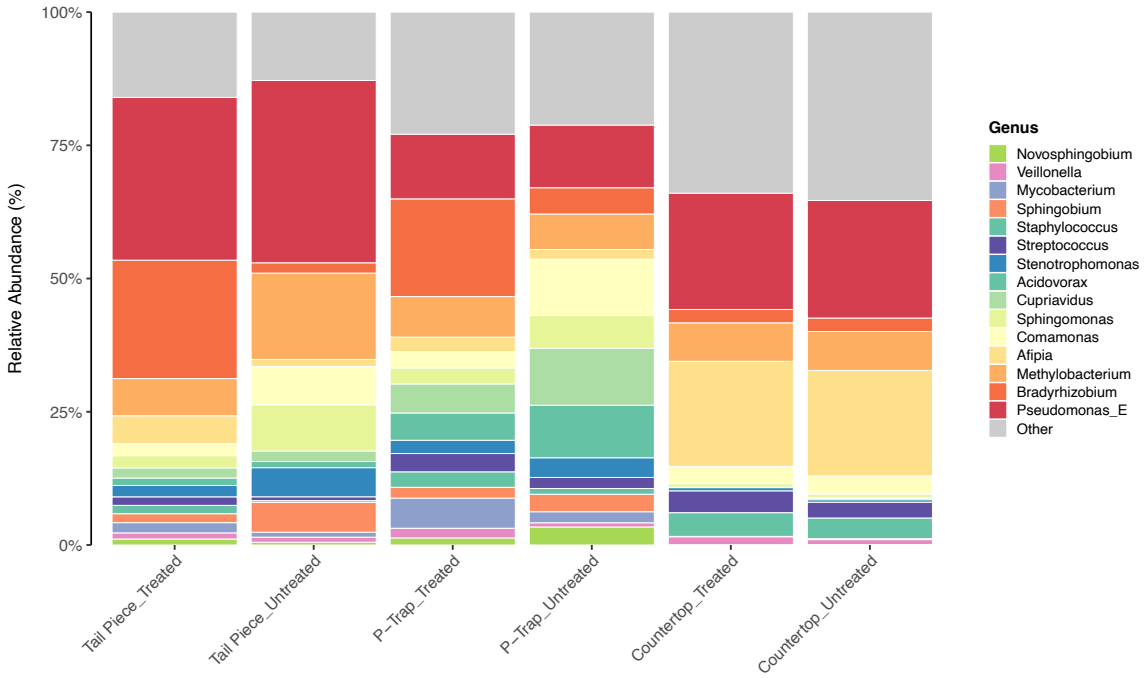

Figure 4. Taxonomic composition of dominant bacterial genera in hospital sink communities. Percent relative abundances of the 15 most abundant bacterial genera across treatment groups and sampling locations.

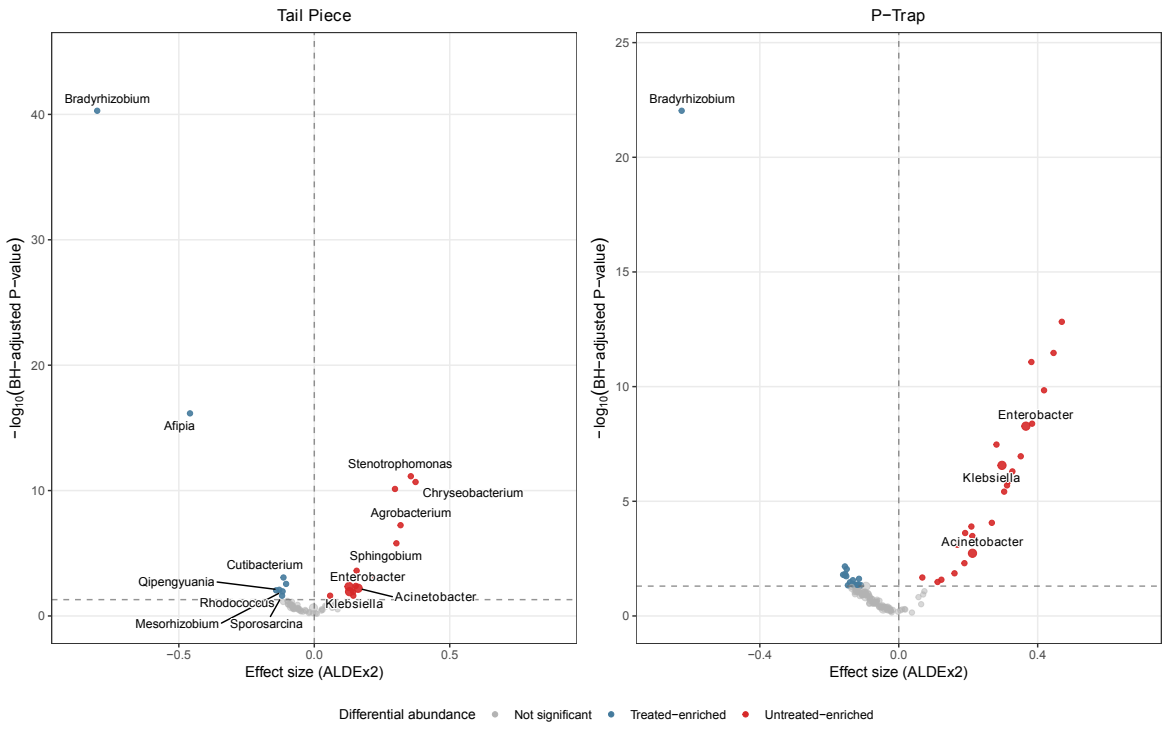

Figure 5. Differentially abundant taxa between treated and untreated samples for the P-trap and tail piece. Calculated with ALDEx2. Effect size > 0: enriched in untreated samples; Effect size < 0: enriched in treated samples. Enlarged dots represent genera with ESKAPEE pathogens. Dashed lines represent significance thresholds.

Tables

Table 1. Differential abundance analysis of bacterial genera in hospital sink samples. ALDEx2 analysis comparing treated versus untreated communities at P-trap and tail piece sampling locations. Analysis performed on genus-level relative abundances. Only genera with ≥ 5% prevalence within each location were included. Results sorted by effect size magnitude. No differentially abundant taxa identified from countertop samples.

* indicates genera with ESKAPEE pathogens

Tail Piece					
Genus	**Effect**	**BH(wi)**	**BH(we)**	**diff.btw**	**Direction**
Bradyrhizobium	-0.801	0	0	-7.268	TREATED
Afipia	-0.459	0	0	-4.226	TREATED
Rhodococcus	-0.141	0.0141	0.0091	-0.832	TREATED
Qipengyuania	-0.129	0.028	0.0082	-0.971	TREATED
Sporosarcina	-0.119	0.0244	0.0464	-0.82	TREATED
Mesorhizobium	-0.117	0.0477	0.0109	-0.732	TREATED
Cutibacterium	-0.114	0.0234	0.0009	-0.785	TREATED
Pelomonas	-0.104	0.0536	0.0028	-0.898	TREATED
Methylobacterium	0.059	0.1714	0.0241	0.434	UNTREATED
Enterobacter *	0.128	0.0177	0.0045	1.014	UNTREATED
Klebsiella *	0.13	0.0234	0.0116	0.984	UNTREATED
Bosea	0.143	0.0245	0.012	0.977	UNTREATED
Microbacterium	0.144	0.0342	0.0241	1.02	UNTREATED
Novosphingobium	0.153	0.004	0.0409	1.366	UNTREATED
Comamonas	0.156	0.0076	0.0002	1.352	UNTREATED
Acinetobacter *	0.162	0.0062	0.0155	1.585	UNTREATED
Brevundimonas	0.211	0.0009	0.005	1.755	UNTREATED
Sphingomonas	0.298	0	0	2.475	UNTREATED
Sphingobium	0.303	0	0	3.09	UNTREATED
Agrobacterium	0.319	0	0	2.259	UNTREATED
Stenotrophomonas	0.356	0	0	3.393	UNTREATED

Chryseobacterium	0.374	0	0	2.929	UNTREATED
P-Trap					
Genus	**Effect**	**BH(wi)**	**BH(we)**	**diff.btw**	**Direction**
Bradyrhizobium	-0.625	0	0	-4.413	TREATED
Bacillus	-0.16	0.0201	0.0159	-0.958	TREATED
Mycobacterium	-0.156	0.0208	0.0169	-1.537	TREATED
Paenibacillus	-0.155	0.0145	0.0069	-1.107	TREATED
Aerococcus	-0.154	0.0252	0.0147	-0.948	TREATED
Afipia	-0.151	0.0185	0.1325	-1.221	TREATED
Rhodococcus	-0.15	0.009	0.0097	-0.873	TREATED
JABCPE02	-0.147	0.0461	0.0869	-0.8	TREATED
Micrococcus	-0.14	0.0341	0.0444	-0.791	TREATED
Paracoccus	-0.132	0.0412	0.0551	-0.717	TREATED
Sporosarcina	-0.132	0.0276	0.0309	-0.826	TREATED
Methylobacterium	-0.131	0.0399	0.3538	-0.81	TREATED
Dermacoccus	-0.129	0.0524	0.046	-0.765	TREATED
Porphyromonas	-0.12	0.0437	0.0622	-0.723	TREATED
Telluria	-0.117	0.043	0.0476	-0.704	TREATED
Vermiphilus	-0.115	0.0467	0.0239	-0.783	TREATED
Fusobacterium	-0.109	0.0457	0.0723	-0.642	TREATED
Phytobacter	0.068	0.2187	0.0211	0.478	UNTREATED
Azonexus	0.112	0.0672	0.033	0.762	UNTREATED
Pseudoxanthomonas_A	0.123	0.0494	0.0263	0.812	UNTREATED
Pedobacter	0.161	0.0206	0.0138	1.151	UNTREATED
Acidovorax	0.169	0.005	0.0008	1.604	UNTREATED
Caulobacter	0.189	0.0057	0.005	1.324	UNTREATED
Cupriavidus	0.191	0.0002	0.0004	1.54	UNTREATED
Xenophilus	0.209	0.0028	0.0001	1.343	UNTREATED
Microbacterium	0.212	0.001	0.0003	1.436	UNTREATED
Acinetobacter *	0.212	0.0018	0.0066	1.851	UNTREATED
Brevundimonas	0.268	0.0001	0.0014	1.97	UNTREATED
Sphingomonas	0.281	0	0	2.067	UNTREATED

Klebsiella *	0.297	0	0	2.386	UNTREATED
Stenotrophomonas	0.304	0	0	2.771	UNTREATED
Variovorax	0.312	0	0	2.734	UNTREATED
Novosphingobium	0.315	0	0	2.839	UNTREATED
Azospira	0.327	0	0	2.423	UNTREATED
Sphingobacterium	0.351	0	0	2.299	UNTREATED
Enterobacter *	0.366	0	0	3.078	UNTREATED
Comamonas	0.382	0	0	3.056	UNTREATED
Agrobacterium	0.384	0	0	2.67	UNTREATED
Bosea	0.418	0	0	3.048	UNTREATED
Chryseobacterium	0.446	0	0	3.535	UNTREATED
Sphingobium	0.47	0	0	4.276	UNTREATED

Tail Piece

Genus	Effect	BH(wi)	BH(we)	diff.btw	Direction
Bradyrhizobium	-0.801	0	0	-7.268	TREATED
Afipia	-0.459	0	0	-4.226	TREATED
Rhodococcus	-0.141	0.0141	0.0091	-0.832	TREATED
Qipengyuania	-0.129	0.028	0.0082	-0.971	TREATED
Sporosarcina	-0.119	0.0244	0.0464	-0.82	TREATED
Mesorhizobium	-0.117	0.0477	0.0109	-0.732	TREATED

Cutibacterium	-0.114	0.0234	0.0009	-0.785	TREATED
Pelomonas	-0.104	0.0536	0.0028	-0.898	TREATED
Methylobacterium	0.059	0.1714	0.0241	0.434	UNTREATED
Enterobacter *	0.128	0.0177	0.0045	1.014	UNTREATED
Klebsiella *	0.13	0.0234	0.0116	0.984	UNTREATED
Bosea	0.143	0.0245	0.012	0.977	UNTREATED
Microbacterium	0.144	0.0342	0.0241	1.02	UNTREATED
Novosphingobium	0.153	0.004	0.0409	1.366	UNTREATED
Comamonas	0.156	0.0076	0.0002	1.352	UNTREATED
Acinetobacter *	0.162	0.0062	0.0155	1.585	UNTREATED
Brevundimonas	0.211	0.0009	0.005	1.755	UNTREATED
Sphingomonas	0.298	0	0	2.475	UNTREATED
Sphingobium	0.303	0	0	3.09	UNTREATED
Agrobacterium	0.319	0	0	2.259	UNTREATED
Stenotrophomonas	0.356	0	0	3.393	UNTREATED
Chryseobacterium	0.374	0	0	2.929	UNTREATED

P-Trap					
Genus	**Effect**	**BH(wi)**	**BH(we)**	**diff.btw**	**Direction**
Bradyrhizobium	-0.625	0	0	-4.413	TREATED
Bacillus	-0.16	0.0201	0.0159	-0.958	TREATED
Mycobacterium	-0.156	0.0208	0.0169	-1.537	TREATED
Paenibacillus	-0.155	0.0145	0.0069	-1.107	TREATED
Aerococcus	-0.154	0.0252	0.0147	-0.948	TREATED
Afipia	-0.151	0.0185	0.1325	-1.221	TREATED
Rhodococcus	-0.15	0.009	0.0097	-0.873	TREATED
JABCPE02	-0.147	0.0461	0.0869	-0.8	TREATED
Micrococcus	-0.14	0.0341	0.0444	-0.791	TREATED
Paracoccus	-0.132	0.0412	0.0551	-0.717	TREATED
Sporosarcina	-0.132	0.0276	0.0309	-0.826	TREATED

Methylobacterium	-0.131	0.0399	0.3538	-0.81	TREATED
Dermacoccus	-0.129	0.0524	0.046	-0.765	TREATED
Porphyromonas	-0.12	0.0437	0.0622	-0.723	TREATED
Telluria	-0.117	0.043	0.0476	-0.704	TREATED
Vermiphilus	-0.115	0.0467	0.0239	-0.783	TREATED
Fusobacterium	-0.109	0.0457	0.0723	-0.642	TREATED
Phytobacter	0.068	0.2187	0.0211	0.478	UNTREATED
Azonexus	0.112	0.0672	0.033	0.762	UNTREATED
Pseudoxanthomonas_A	0.123	0.0494	0.0263	0.812	UNTREATED
Pedobacter	0.161	0.0206	0.0138	1.151	UNTREATED
Acidovorax	0.169	0.005	0.0008	1.604	UNTREATED
Caulobacter	0.189	0.0057	0.005	1.324	UNTREATED
Cupriavidus	0.191	0.0002	0.0004	1.54	UNTREATED
Xenophilus	0.209	0.0028	0.0001	1.343	UNTREATED
Microbacterium	0.212	0.001	0.0003	1.436	UNTREATED

Acinetobacter *	0.212	0.0018	0.0066	1.851	UNTREATED
Brevundimonas	0.268	0.0001	0.0014	1.97	UNTREATED
Sphingomonas	0.281	0	0	2.067	UNTREATED
Klebsiella *	0.297	0	0	2.386	UNTREATED
Stenotrophomonas	0.304	0	0	2.771	UNTREATED
Variovorax	0.312	0	0	2.734	UNTREATED
Novosphingobium	0.315	0	0	2.839	UNTREATED
Azospira	0.327	0	0	2.423	UNTREATED
Sphingobacterium	0.351	0	0	2.299	UNTREATED
Enterobacter *	0.366	0	0	3.078	UNTREATED
Comamonas	0.382	0	0	3.056	UNTREATED
Agrobacterium	0.384	0	0	2.67	UNTREATED
Bosea	0.418	0	0	3.048	UNTREATED
Chryseobacterium	0.446	0	0	3.535	UNTREATED
Sphingobium	0.47	0	0	4.276	UNTREATED

554

555 **Supplementary Material**

Table S1. Significance results for per-week volatility analysis. P-values are calculated based on PERMANOVA with week as the sole predictor of Aitchison distance. * = $p < 0.05$ (significant), ** = $p < 0.01$ (highly significant), *** = $p < 0.001$ (very highly significant), — = insufficient data

Week	Tail Piece	P-Trap	Countertop
1	0.022*	0.031*	0.189
2	0.002**	0.003**	0.134
3	-	0.08	0.104
4	0.052	0.864	-
5	0.001**	-	0.595
6	0.001**	0.908	0.56
7	0.247	-	0.182
8	0.2	-	0.836
9	0.2	0.019*	0.844
10	0.078	0.091	0.896
11	0.155	0.186	0.93
12	0.001**	0.12	0.672
13	0.085	0.002**	0.845
14	0.005**	0.004**	0.011*
15	0.12	0.07	0.109
16	0.047*	0.424	0.46
17	0.001**	0.772	-
18	0.663	0.007**	0.198
20	0.061	0.001**	0.773
21	0.001**	0.001**	0.296
22	0.003**	0.007**	0.786
24	0.001**	0.001**	0.737
26	0.001**	0.004**	0.216
27	0.155	0.135	0.465
28	0.001**	0.001**	0.404
29	0.001**	0.3	0.41

30	-	0.028*	0.142
31	0.018*	-	0.946
32	0.005**	0.008**	0.945
33	0.001**	-	0.562
34	0.002**	-	0.506
35	0.001**	-	0.327

561